Available online at www.sciencedirect.com

ScienceDirect

Mendeleev Commun., 2018, **28**, 659–660

Mendeleev Communications

Electrochemical insertion of sodium into nanostructured materials based on germanium

Ilya M. Gavrilin,[a] Vladimir A. Smolyaninov,[a] Alexey A. Dronov,[a] Sergei A. Gavrilov,[a] Alexey Yu. Trifonov,[a,b] Tatiana L. Kulova,*[c] Anna A. Kuz'mina[c] and Alexander M. Skundin[c]

[a] *National Research University of Electronic Technology, 124498 Zelenograd, Moscow, Russian Federation*
[b] *F. V. Lukin State Research Institute of Physical Problems, 124498 Zelenograd, Moscow, Russian Federation*
[c] *A. N. Frumkin Institute of Physical Chemistry and Electrochemistry, Russian Academy of Sciences, 119071 Moscow, Russian Federation. Fax: +7 495 952 5308; e-mail: tkulova@mail.ru*

DOI: 10.1016/j.mencom.2018.11.034

The filamentary nanostructures of composition $Ge_{0.91}In_{0.09}$ were synthesized from the aqueous solution by electrolysis. It has been demonstrated that at the low current density, the reversible capacity of sodium insertion into the composition is about 590 mAh g^{-1}, which corresponds to $Na_{1.73}Ge_{0.91}In_{0.09}$ alloy.

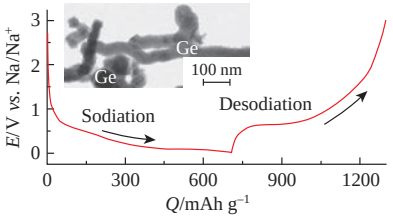

Sodium-ion batteries are among the most promising candidates to replace the lithium-ion batteries since they work on the same principle, whereas sodium is low cost and abundant metal as compared to lithium. While such a battery is being charged, the alkali metal ions (sodium or lithium) are extracted from a positive electrode material and introduced into the matrix of negative electrode. These processes are reversed during the discharge.

Various materials capable of forming alloys or intercalation compounds with sodium, *e.g.*, tin,[1,2] antimony[3–8] and its composites with carbon,[9–11] and also alloys of antimony,[12–14] can be employed as a negative electrode in the sodium-ion battery. The intercalation capacity of such materials is not high and ranges from 200 to 400 mAh g^{-1}. At the same time, there are much more interesting materials that can form alloys with fairly high sodium content. For instance, germanium is able to alloy with sodium up to composition of Na_3Ge.[15] This means that the theoretical specific capacity of germanium with due account for Faraday lows can reach the value of 1107 mAh g^{-1}. The formation possibility for alloys enriched with sodium ($Na_{1.6}Ge$) has been already proved experimentally,[16] however without any data on prolonged cycling.

Germanium nanostructures can be synthesized by various methods, *viz.*, crystallization from a supercritical fluid,[16] chemical deposition of their gas phase,[17] magnetron sputtering,[18] and electron beam evaporation.[19] However, the structures obtained by those methods possess a low intercalation capacity for the sodium insertion (much lower than the theoretical value), as well as reveal a large degradation during cycling.

In the present work, the germanium samples were prepared by electrolysis in an aqueous solution of germanium oxide on a titanium substrate with a previously deposited array of spherical indium nanoparticles.† This method was completely described in our previous report.[20] Electrochemical tests were carried out in three-electrode cells.‡

The scanning electron microscopy (SEM) study of germanium morphology revealed that the synthesized samples represented filamentary structures with the diameter from 30 to 80 nm and length of 1 μm (Figure 1). The average thickness of the germanium layer was about 850 nm. Taking into account the energy-dispersive X-ray analysis data, one can conclude that the formed filamentary structures represent Ge containing 9 at% of In. The presence of In in the structure is caused by its dissolution in Ge during the growth of structures thus forming $Ge_{0.91}In_{0.09}$ alloy.

The charge–discharge curves [Figure 2(*a*)] recorded during the introduction–extraction of sodium into germanium suggest an opportunity to apply this material as the anode in a sodium-ion battery due to the prolonged plateau in the potential region of 600–700 mV recorded on the discharge curve and the reversible capacity close to its theoretical value. Sodium is known to be capable of forming alloys with indium,[21] while the theoretical reversible capacity of Na_2In alloy is 469 mAh g^{-1}. Taking into

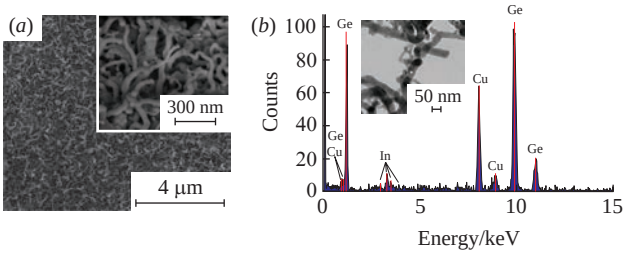

Figure 1 (*a*) SEM-image and (*b*) energy-dispersive X-ray analysis of Ge alloy.

† After the application of In, the samples were annealed *in vacuo* at 150 °C for 10 min. The solution contained GeO_2 (0.05 M), K_2SO_4 (0.5 M) as the supporting electrolyte, and succinic acid (0.5 M) as the buffering additive. The solution pH was adjusted to 6.5 by addition of NH_4OH. The deposition process was performed at 90 °C at the potential of –1.3 V (SCE).

‡ The counter and reference electrodes were manufactured from sodium metal rolled on a nickel grid substrate. The $NaClO_4$ (1 M) in a mixture of ethylene carbonate–diethyl carbonate–dimethyl carbonate (1:1:1, v/v) was used as the electrolyte. The mass loading for In–Ge electrodes investigated was 0.1 mg cm^{-2}.

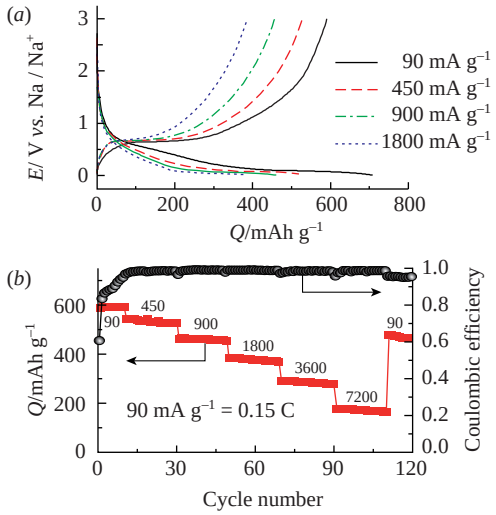

Figure 2 (*a*) Charge–discharge curves and (*b*) change in the reversible capacity of the germanium-based electrode during the insertion–extraction of sodium at different current densities. Current values are expressed in mA g^{-1}.

account the fact that sodium can form alloys with germanium up to the composition Na_3Ge,[15] the composition $Ge_{0.91}In_{0.09}$ can produce alloy $Na_{2.91}Ge_{0.91}In_{0.09}$ with the specific capacity of 1020 mAh g^{-1}.

Thus, the reversible capacity of 590 mAh g^{-1} recorded at a low current density (0.15 C) for the nanostructured germanium-based sample can correspond to the composition $Na_{1.73}In_{0.09}Ge_{0.91}$. An increased current density leads to a decrease in the reversible capacity, which is caused by the slow diffusion of sodium ions in the solid phase. However, even at a fairly high current density of 7200 mA g^{-1} (12 C), the reversible capacity was as much as 180 mAh g^{-1}. The electrodes were characterized by stable cycling with simultaneous rather high capacity. After 120 charge–discharge cycles, the reversible capacity was 80% of its initial value [Figure 2(*b*)]. The coulombic efficiency of first cycle was about 0.61, which is related to the well-known phenomenon of solid electrolyte interphase formation. This efficiency has reached 0.98 up to 12th cycle and remained constant during further cycling. Such stable cycling of the germanium-based electrodes can be explained by the unique filamentary morphology of synthesized germanium and the change in the mechanical properties of thread-like structures due to the dissolution of indium in germanium during the synthesis. Since the atomic radius of indium is 36% larger than that of germanium, the $Ge_{0.91}In_{0.09}$ alloy can be considered as a prestrained material. According to the known data,[22] such materials are less susceptible to degradation during the insertion–extraction of alkali metal ions. Critical mechanical failure during the insertion of alkali metal was observed for materials with a feature size of more than 1.2 μm.[22]

Cyclic voltamograms of germanium-based electrode at different potential scan rates are shown in Figure 3. The process of sodium intercalation is described by a clear peak at the potentials of 50–60 mV, while the extraction process is described by a response

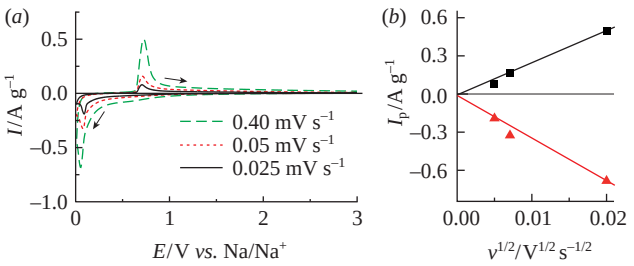

Figure 3 (*a*) Cyclic voltamograms of germanium-based electrode during the insertion–extraction of sodium and (*b*) peak current *vs.* potential scan rate.

peak at the potentials of 700–710 mV. The dependences of peak currents on the square root of potential scan rate are linear and go through the origin of coordinates, which evidences the diffusion process of sodium insertion–extraction into germanium.

Therefore, this work revealed the nanostructured germanium obtained by electrochemical deposition from an aqueous solution using In nanoparticles as the crystallization centers. This material composition is $Ge_{0.91}In_{0.09}$ and it is characterized by the reversible capacity for the sodium insertion of about 590 mAh g^{-1}, which overcomes the results achieved previously. The filamentary morphology of synthesized material and the presence of indium in germanium ensure its stable cycling and the ability to withstand the high charge–discharge currents. The absence of any significant degradation of sodium enriched materials during cycling distinguishes this new material from the described germanium nanostructured samples. Its stability during cycling can be explained by the unique filamentary morphology of germanium nanostructures and also by the changed mechanical properties of germanium due to the formation of alloy with indium.

This work was carried out within the State Assignment on Applied Research from the Ministry of Education and Science of the Russian Federation to the National Research University of Electronic Technology (MIET) (assignment no. 16.2653.2017/4.6).

References

1 M. Shimizu, H. Usui and H. Sakaguchi, *J. Power Sources*, 2014, **248**, 378.
2 Y. C. Lu, C. Ma, J. Alvarado, T. Kidera, N. Dimov, Y. S. Meng and S. Okada, *J. Power Sources*, 2015, **284**, 287.
3 Y. Wang, D. Su, C. Wang and G. Wang, *Electrochem. Commun.*, 2013, **29**, 8.
4 Y.-X. Wang, Y.-G. Lim, M.-S. Park, S.-L. Chou, J. H. Kim, H.-K. Liu, S.-X. Dou and Y.-J. Kim, *J. Mater. Chem. A*, 2014, **2**, 529.
5 D. Su, H.-J. Ahn and G. Wang, *Chem. Commun.*, 2013, **49**, 3131.
6 Y. Zhang, J. Xie, S. Zhang, P. Zhu, G. Cao and X. Zhao, *Electrochim. Acta*, 2015, **151**, 8.
7 X. Wu, W. Wu, Y. Zhou, X. Huang, W. Chen and Q. Wang, *Powder Technol.*, 2015, **280**, 119.
8 Y. Xu, E. M. Lotfabad, H. Wang, B. Farbod, Z. Xu, A. Kohandehghan and D. Mitlin, *Chem. Commun.*, 2013, **49**, 8973.
9 L. Wu, D. Buchholz, D. Bresser, L. G. Chagas and S. Passerini, *J. Power Sources*, 2014, **251**, 379.
10 Z. Yan, L. Liu, J. Tan, Q. Zhou, Z. Huang, D. Xia, H. Shu, X. Yang and X. Wang, *J. Power Sources*, 2014, **269**, 37.
11 L. Wu, D. Bresser, D. Buchholz and S. Passerini, *J. Electrochem. Soc.*, 2015, **162**, A3052.
12 J. Lee, Y.-M. Chen, Y. Zhu and B. D. Vogt, *ACS Appl. Mater. Interfaces*, 2014, **6**, 21011.
13 S.-M. Oh, J.-Y. Hwang, C. S. Yoon, J. Lu, K. Amine, I. Belharouak and Y.-K. Sun, *ACS Appl. Mater. Interfaces*, 2014, **6**, 11295.
14 K.-N. Jung, J.-Y. Seong, S.-S. Kim, G.-J. Lee and J.-W. Lee, *RSC Adv.*, 2015, **5**, 106252.
15 Y. Wang, P. Wang, D. Zhao, B. Hu, Y. Dua, H. Xua and K. Chang, *Calphad*, 2012, **37**, 72.
16 X. Lu, E. R. Adkins, Y. He, L. Zhong, L. Luo, S. X. Mao, C.-M. Wang and B. A. Korgel, *Chem. Mater.*, 2016, **28**, 1236.
17 A. Kohandehghan, K. Cui, M. Kupsta, J. Ding, E. M. Lotfabad, W. P. Kalisvaart and D. Mitlin, *Nano Lett.*, 2014, **14**, 5873.
18 L. Baggetto, J. K. Keum, J. F. Browning and G. M. Veith, *Electrochem. Commun.*, 2013, **34**, 41.
19 P. R. Abel, Y.-M. Lin, T. de Souza, C.-Y. Chou, A. Gupta, J. B. Goodenough, G. S. Hwang, A. Heller and C. B. Mullins, *J. Phys. Chem. C*, 2013, **117**, 18885.
20 I. M. Gavrilin, D. G. Gromov, A. A. Dronov, S. V. Dubkov, R. L. Volkov, A. Yu. Trifonov, N. I. Borgardt and S. A. Gavrilov, *Semiconductors*, 2017, **51**, 1067 (*Fiz. Tekh. Poluprovodnikov*, 2017, **51**, 1110).
21 S. C. Sevov and J. D. Corbett, *J. Solid State Chem.*, 1993, **103**, 114.
22 J. Gu, S. M. Collins, A. I. Carim, X. Hao, B. M. Bartlett and S. Maldonado, *Nano Lett.*, 2012, **12**, 4617.

Received: 3rd May 2018; Com. 18/5564